IEEE Access
Multidisciplinary | Rapid Review | Open Access Journal

Received May 8, 2018, accepted June 10, 2018, date of publication July 25, 2018, date of current version August 20, 2018.

Digital Object Identifier 10.1109/ACCESS.2018.2852323

Multi-Step Prediction of Physiological Tremor With Random Quaternion Neurons for Surgical Robotics Applications

YUBO WANG[1], (Member, IEEE), SIVANAGARAJA TATINATI[2], (Member, IEEE), KABITA ADHIKARI[3], (Member, IEEE), LIYU HUANG[1], KIANOUSH NAZARPOUR[4], (Senior Member, IEEE), WEI TECH ANG[5], (Member, IEEE), AND KALYANA C. VELUVOLU[6], (Senior Member, IEEE)

[1]School of Life Science and Technology, Xidian University, Xi'an 710071, China
[2]School of Electrical and Electronics Engineering, Nanyang Technological University, Singapore 639798
[3]School of Electrical and Electronic Engineering, Newcastle University, Newcastle upon Tyne NE1 7RU, U.K.
[4]School of Electrical and Electronic Engineering and the Institute of Neuroscience, Newcastle University, Newcastle upon Tyne NE1 7RU, U.K.
[5]School of Mechanical and Aerospace Engineering, Nanyang Technological University, Singapore 639798
[6]School of Electronics Engineering, College of IT Engineering, Kyungpook National University, Daegu 720701, South Korea

Corresponding author: Kalyana C. Veluvolu (veluvolu@knu.ac.kr)

The work of Y. Wang was supported in part by the Fundamental Research Funds for the Central Universities, Xidian University, under Grant JB181205, and in part by the National Natural Science Foundation of China under Grant 81701787. The work of K. C. Veluvolu was supported in part by the National Research Foundation (NRF) of Korea through the Ministry of Education, Science and Technology under Grants NRF- 2017R1A2B2006032 and NRF-2018R1A6A1A03025109, and in part by the BK21 Plus Project through the Ministry of Education, South Korea, under Grant 21A20131600011.

ABSTRACT Digital filters are employed in hand-held robotic instruments to separate the concomitant involuntary physiological tremor motion from the desired motion of micro-surgeons. Inherent phase-lag in digital filters induces phase distortion (time-lag/delay) into the separated tremor motion and it adversely affects the final tremor compensation. Owing to the necessity of digital filters in hand-held instruments, multi-step prediction of physiological tremor motion is proposed as a solution to counter the induced delay. In this paper, a quaternion variant for extreme learning machines (QELMs) is developed for multi-step prediction of the tremor motion. The learning paradigm of the QELM integrates the identified underlying relationship from 3-D tremor motion in the Hermitian space with the fast learning merits of ELMs theories to predict the tremor motion for a known horizon. Real tremor data acquired from micro-surgeons and novice subjects are employed to validate the QELM for various prediction horizons in-line with the delay induced by the order of digital filters. Prediction inferences underpin that the QELM method elegantly learns the cross-dimensional coupling of the tremor motion with random quaternion neurons and hence obtained significant improvement in prediction performance at all prediction horizons compared with existing methods.

INDEX TERMS Surgical robotics, physiological tremor, multi-step prediction, random quaternion neurons, extreme learning machines.

I. INTRODUCTION

Minimally-invasive surgical procedures require compensation of micro-surgeon's intrinsic physiological tremor which is concomitant with the desired motion [1]–[3]. Physiological tremor motion has amplitude ranges typically from 50μm to 100μm and displays multiple dominant spectral components in the frequency band of 6Hz to 20Hz [4]–[6]. The requirement of precision and dexterity at micrometer range movements in micro-surgical procedures (about 10μm) lead to the advent of various smart surgical robotic instruments/techniques [7]. Hand-held micro-surgical robotic instruments such as the "Micron" [8] and the "iTrem" [9], [10] among the developed surgical robotic instruments gained a great-deal of attention lately due to their ability of

augmenting the required precision into the normal surgical-flow by compensating the physiological tremor in real-time.

The working principle of a typical smart hand-held instrument is depicted in Fig. 1. The instrument comprises of a sensing unit which houses inertial sensors for sensing the micro-meter range motions; and a compensation unit with piezo-electric actuators to perform manipulations on sub-millimeter range motions. As the voluntary motion and the tremor motion share distinct frequency characteristics, these instruments employ a digital filter at the modeling unit to separate the voluntary motion from its concomitant tremor motion acquired with the sensing unit, as shown in Fig. 1(a). This separated tremor motion is then provided to the compensation unit for manipulating the tip-position and hence compensate the tremor motion [9].

Experiments conducted with the hand-held instruments for tremor compensation concluded that the final tremor compensation is reliable if and only if the performed manipulations are in-phase with the tremor motion (ideally zero-phase lag). However, inherent phase delay of the digital filters employed at the modeling unit resulted in phase-distorted (in time domain phase distortion causes time-lag or delay) tremor motion. The final-tremor compensation efficacy of hand-held instruments with the delayed tremulous motion is no better than the uncompensated motion. To illustrate the effect of delay on final tremor compensation, manipulated tip-position with and without the presence of delay (3rd order low-pass filter delay - 40ms) on a typical tremor motion is depicted in Fig. 1 (a) (sensing unit and compensation unit schema's are considered same as in [9]). Furthermore, the range of delay increases with increase in filter order, as shown in Fig. 1 (b). Therefore, a prediction algorithm that mitigates the effect of phase delay due to the digital filters by accurately predicting the non-stationary natured physiological tremor motion in real-time is necessary to enhance the hand-held instrument compensation capabilities.

Conventional signal processing methods such as autoregressive (AR) model, and truncated Fourier series (the eighted Fourier linear combiner (WFLC) and the band-limited Fourier linear combiner (BMFLC)) with Kalman filter are proposed for multi-step prediction of physiological tremor motion [11], [12]. Recently, a quaternion variant for WFLC (QwFLC) is proposed to exploit the cross-dimensional coupling across x, y, and z axes in tremor motion and thus enhance single-step tremor prediction accuracy [13]. For predicting future samples, all these methods assume that the tremor signal characteristics remain constant over the prediction horizon. A future value is then obtained by iterating over the signal model without receiving any real measurements. Since tremor motion is non-stationary in nature, this assumption does not hold true for long prediction horizons [12]. To overcome this assumption, tremor prediction methods based on machine learning techniques (least squares support vector machines (LSSVM-1D) [12] and multi-dimensional variant of extreme learning machines (ELM-3D) [14]) are developed. Results showed that, at all prediction horizons, LSSVM-1D and ELM-1D (one dimensional ELM) yield better prediction inference compared to Kalman filter based adaptive algorithm [12].

Tremor motion generally resides in three-dimensional (3D) space and has cross-dimensional coupling. Thus, tremor prediction method must equip with the following abilities to manipulate the tip position accurately in 3D-space : 1) predict the tremor motion in all three axes simultaneously; 2) capable of utilizing the pertained cross-dimensional coupling; and 3) less computationally demanding. Prediction of the tremor motion in 3D space with LSSVM-1D and ELM-1D methods can be achieved only by implementation of these methods in each dimension separately, which does not fit into the above mentioned abilities. Formulation of a prediction model in 3D space with these methods forces the optimization problem to solve for each output-dimension separately, thus cross-dimensional coupling is not considered. Furthermore, while optimizing for 3D models, the computational complexity of LSSVM-3D is three times the computational requirement of LSSVM-1D whereas the innate structure of ELM keeps the computational complexity of ELM-3D similar to ELM-1D.

Although ELM-3D is suitable for surgical robotic applications owing to its generalization capabilities and less computational complexity, it lacks exploiting cross-dimensional coupling. Furthermore, in the random feature space formulated with 3D measurements, ELM-3D can not regularize the influence of correlation information obtaining from other axes accurately to improve the overall prediction inference. For various tracking applications, it has been shown that modeling multi-dimensional data in the Hermitian space as quaternions brings an elegant way of handling the cross-dimensional coupling compared to real-valued multi-dimensional modeling [15], [16]. In addition, tremor modeling (single-step prediction) results obtained with QwFLC yielded nearly 60% improvement in accuracy compared to its real-valued counterpart [13]. Motivated by these developments, in this work, a quaternion variant for ELM (QELM) is developed for multi-step prediction of physiological tremor.

The QELM combines the merit of fast learning from ELM and utilizes the cross-dimensional coupling from quaternion signal modeling. A proof-of-concept with preliminary results obtained for modeling (single-step prediction) of tremor motion with the QELM is reported in [17]. In this work, the formulated multi-step prediction model with quaternion variant is detailed. This prediction model is evaluated with the tremor data collected from five healthy subjects and five micro-surgeons while performing typical micro-surgical tasks such as pointing task and tracing tasks. A comparison analysis is performed on the real-tremor data among ELM-1D, LSSVM-1D, QwFLC, ELM-3D, and QELM for the prediction horizons in-line with the delay introduced by low-pass filters in the instrument, i.e., 40ms, 60ms. Results showed that the QELM significantly improves the tremor prediction accuracy compared to the other existing methods.

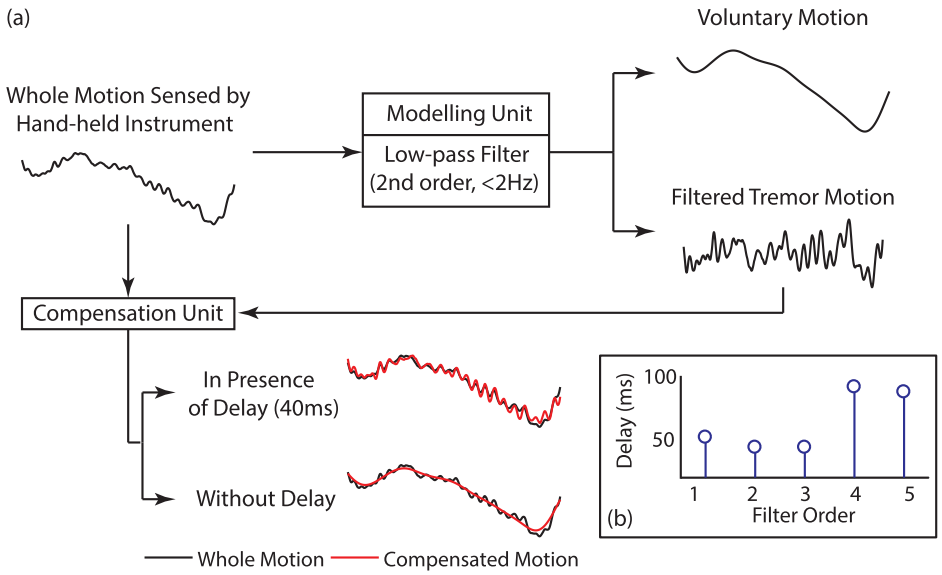

FIGURE 1. Schematic diagram of a typical hand-held robotic instrument a) working principle and effect of phase delay; b) delay due to the digital filter.

Analysis conducted on the run-time complexity showed that the QELM method consumes less computational resources (less than 1ms) which highlights the advantages of the QELM for tremor prediction in surgical robotic applications.

The paper is organized as follows. In Section II, the background theory of QELM and the paradigm for multi-step prediction of physiological tremor are provided. Section III presents description of the tremor data used in this work and the performance evaluation of the proposed methods along with the inferences. Discussions and conclusions are provided in Sections IV and V respectively.

II. MULTI-STEP PREDICTION OF PHYSIOLOGICAL TREMOR WITH RANDOM QUATERNION NEURONS

Physiological tremor motion acquired with hand-held instruments at time instant t in the 3-D space (x, y, *and* z axes) can be represented by its corresponding axial components $d_{(t,x)}$, $d_{(t,y)}$ and $d_{(t,z)}$. To utilize cross dimensions information, a pure quaternion variable is formulated with the three axial components, can be given as:

$$\tilde{x}_t = id_{(t,x)} + jd_{(t,y)} + kd_{(t,z)}. \tag{1}$$

Multi-step prediction of physiological tremor in the Hermitian space ($\mathcal{H}$) can be considered as a classical learning problem of estimating an unknown underlying relation between the elements of an input feature space ($\boldsymbol{S} \in \mathcal{H}^m$) and elements of an target space ($\boldsymbol{T} \in \mathcal{H}^n$). The elements in the input feature space are formulated as quaternions of the tremor signal (give in (1)), can be given as $\tilde{\boldsymbol{x}}_t = [\tilde{x}_t, \tilde{x}_{t-1}, \cdots, \tilde{x}_{t-p}]$, where p is the order of the modeling. The elements in target space corresponding to the each element in input feature space $\tilde{\boldsymbol{x}}_t$ is q samples ahead of current sample, can be given as $\tilde{y}_t = \tilde{x}_{t+q}$, where the q is the prediction horizon. The formulated input vector and target vector

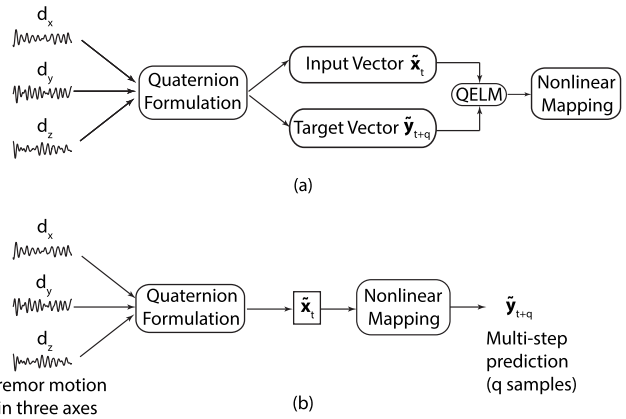

FIGURE 2. QELM for modeling (a) and prediction (b) of physiological tremor.

with the training data are provided to the QELM for learning a nonlinear map that better represents the relationship between the input feature space and the target vector space, as shown in Fig.2(a). In the testing phase, the input vector in quaternion domain will be formulated initially from the unseen tremor data, as shown in Fig.2(b). The formulated input vector will be provided to the nonlinear map attained in the training phase to yield the q samples ahead predicted value of the tremor signal.

RANDOM QUATERNION NEURONS: QUATERNION EXTREME LEARNING MACHINES (QELM)

Extreme learning machine (ELM) is one of the effective training procedures to tune the single hidden layer feed-forward networks (SLFN) parameters [19]. It first assigns the input weights and hidden layer bias randomly, then the output weights can be solved by using simple generalized inverse

operation. For a set of $\tilde{N}$ distinct samples $\mathcal{S} = \{(\boldsymbol{s}_i, \boldsymbol{t}_i) \mid \boldsymbol{s}_i \in \mathbb{R}^m,\ \boldsymbol{t}_i \in \mathbb{R}^n; i = 1, \cdots, \tilde{N}\}$ with $\boldsymbol{s}_i = [s_{i,1}, \cdots, s_{i,m}]^T$ as input vector, $\boldsymbol{t}_i = [t_{i,1}, \cdots, t_{i,n}]^T$ as its corresponding target vector, ELM finds the mapping between the input and its corresponding target through the following equation:

$$\boldsymbol{o}_j = f_L(\mathcal{S}) = \sum_{i=1}^{L} \beta_i g_i(w_i \boldsymbol{s}_j + b_i), \quad \text{for } j = 1, \cdots, \tilde{N} \tag{2}$$

where $\boldsymbol{o}_j$ represents the predicted signal with the ELM, w_i is the input weights connecting the i-th hidden unit to the input vector $\boldsymbol{s}_i$, b_i is the hidden layer bias and β_i denotes output layer weights. The universal approximation of ELM requires the activation function $g_i(\bullet) : \mathbb{R} \to \mathbb{R}$ to be a bounded non-constant piecewise continuous function [18]. During the training phase, the input weights $w_i \in \mathbb{R}^m$ and the hidden unit bias $b_i \in \mathbb{R}$ are randomly assigned according to any continuous probability distribution. Combining all $\tilde{N}$ equations in Eq.2, we have the following linear system

$$\mathbf{H}\boldsymbol{\beta} = \mathbf{T} \tag{3}$$

where $\mathbf{H}$ is a $(L \times \tilde{N})$ matrix with each row represents the value of a input being activated through L hidden units. $\mathbf{T}$ contains all $\tilde{N}$ target vector for each input. Thus, the output weight matrix $\boldsymbol{\beta}$ can be obtained as

$$\boldsymbol{\beta} = \boldsymbol{H}^{\dagger}\boldsymbol{T} \tag{4}$$

where † denotes the Moore-Penrose generalized matrix inversion. For detailed description about ELM, refer to [19].

RANDOM QUATERNION NEURONS FORMULATION

Quaternion representation of tremor signal is a natural extension of the traditionally employed complex analysis to handle 3D or 4D signals. A general quaternion variable $q \in \mathbb{H}$ is defined as

$$q = q_r + iq_i + jq_j + kq_k$$

where $\{q_r, q_i, q_j, q_k\} \in \mathbb{R}$ and i, j, and k are imaginary units obeying the following rules:

$$ij = k, \quad jk = i, \ ki = j,$$
$$i^2 = j^2 = k^2 = ijk = -1.$$

A quaternion variable with $q_r = 0$ is called a pure quaternion. In this work, we model the tremor signal in the 3D space, i.e., as only pure quaternions. The conjugate of a quaternion variable q is defined as $q^* = q_r - iq_i - jq_j - kq_k$ and the norm of a quaternion variable is given as:

$$\|q\| = \sqrt{qq^*} = \sqrt{q_r^2 + q_i^2 + q_j^2 + q_k^2}.$$

Given N distinct quaternion tremor samples in Hermitian space, given as $\{(\tilde{\boldsymbol{x}}_t, \tilde{\boldsymbol{y}}_t) | \ \tilde{\boldsymbol{x}}_t \in \mathbb{H}^m,\ \tilde{\boldsymbol{y}}_t \in \mathbb{H}^n;\ t = 1, \cdots, \tilde{N}\}$, where $\mathbb{H}$ denotes the quaternion filed. $\tilde{\boldsymbol{x}}_t = [\tilde{x}_{t,1}, \cdots, \tilde{x}_{t,m}]$ and $\tilde{\boldsymbol{y}}_t = [\tilde{y}_{t,1}, \cdots, \tilde{y}_{t,n}]$ are the quaternion valued feature vector and its corresponding target vector at time instant t. Each element in $\tilde{\boldsymbol{x}}_t$ and $\tilde{\boldsymbol{y}}_t$ is a quaternion variable. QELM finds a mapping between the feature vector and the target vector as:

$$\tilde{\boldsymbol{o}}_t = \sum_{i=1}^{L} \tilde{\beta}_i f_i(\tilde{w}_i \tilde{x}_t + \tilde{b}_i) \quad \text{for } t = 1, \cdots, \tilde{N} \tag{5}$$

where $\tilde{\boldsymbol{o}}_t$ is the predicted value through the QELM, $\tilde{\boldsymbol{w}}_i \in \mathbb{H}^m$ and $\tilde{b}_i \in \mathbb{H}$ are the weight and bias of a quaternion hidden unit connecting the i-hidden units to a input vector, $f(\bullet) : \mathbb{H} \to \mathbb{H}$ is the activation function of a hidden unit and L represent the total number of hidden units.

There are three main steps in the implementation of the QELM method. Firstly, random samples of the weights and bias value of each hidden unit are obtained according to a continuous probability distribution function. The random sampling of weights and bias of the hidden unit in quaternion domain can be considered as generating random points on a hypersphere as detailed in [20]. The input vector is then provided to each hidden unit to transform the input into random feature space by a nonlinear activation function. In line with the real-valued ELM, the activation function $f(\bullet)$ is a bounded non-constant piecewise continuous function. It has been shown that the function in $\mathbb{H}$ space that satisfies the local analyticity condition (LAC) can be employed as the activation function in a neural network [16], [21]. Thus, in this work, the $\tanh(\cdot)$ function is employed as the nonlinear activation in QELM. For a typical quaternion input q, the activation function can be given as

$$\tanh(q) = \frac{e^q - e^{-q}}{e^q + e^{-q}}.$$

After mapping the input vector into the random feature space with the above formulation, as the final step, the output layer weights are computed as follows:

$$\tilde{\mathbf{H}}\tilde{\boldsymbol{\beta}} = \tilde{\mathbf{T}} \tag{6}$$

where $\tilde{\mathbf{H}} \in \mathbb{H}^{\tilde{N} \times L}$ and is given as

$$\tilde{\mathbf{H}} = \begin{bmatrix} f_1(\tilde{w}_1 \boldsymbol{x}_1 + \tilde{b}_1) & \cdots & f_L(\tilde{w}_L x_1 + \tilde{b}_L) \\ \vdots & \vdots & \cdots \\ f_1(\tilde{w}_1 x_N + \tilde{b}_1) & \cdots & f_L(\tilde{w}_L x_{\tilde{N}} + \tilde{b}_L) \end{bmatrix} \tag{7}$$

with the output layer weights $\tilde{\boldsymbol{\beta}} \in \mathbb{H}^{L \times n}$ and $\tilde{\mathbf{T}} = [\tilde{y}_1, \cdots, \tilde{y}_{\tilde{N}}]^T$. Similar to the real-valued ELM, the norm of $\tilde{\boldsymbol{\beta}}$ needs to be minimized to give better generation performance of the QELM. Thus, the minimum norm least squares solutions is employed to solve (6) [22] The minimum norm least square solution of $\tilde{\boldsymbol{\beta}}$ is given as:

$$\tilde{\boldsymbol{\beta}} = \tilde{\boldsymbol{H}}^{\dagger}(\tilde{\boldsymbol{H}}\tilde{\boldsymbol{H}}^{\dagger})^{-1}\tilde{\boldsymbol{T}} \tag{8}$$

where $\tilde{\boldsymbol{H}}^{\dagger}$ is the Hermitian adjoint matrix of $\tilde{\boldsymbol{H}}$ with each element defined as $\tilde{H}_{i,j} = \tilde{H}^*_{j,i}$. The solution of a quaternion matrix equation given in (8) uses the fact that the number of columns is larger then the number of rows in $\tilde{\boldsymbol{H}}$, *i.e.* $L \ll \tilde{N}$. In the case of $L \gg \tilde{N}$, the above solution is given as $\tilde{\boldsymbol{\beta}} = (\tilde{\boldsymbol{H}}^{\dagger}\tilde{\boldsymbol{H}})^{-1}\tilde{\boldsymbol{H}}^{\dagger}\tilde{\boldsymbol{T}}$. In the implementation

of QELM, we can always ensure the relation $L \ll \tilde{N}$ is satisfied by choosing the number of hidden units L to be less than the available training samples. The necessary and sufficient condition for a quaternion matrix to be invertible has been established in [22].

III. RESULTS

A. PHYSIOLOGICAL TREMOR DATABASE

Physiological tremor motion was recorded with the Micro Motion Sensing System ($M2S2$) and a sensorized stylus with a reflector ball at its tip [23]. The $M2S2$ system provides measurement in a $10 \times 10 \times 10\, mm^3$ workspace, with a resolution of 0.7 μm and minimum accuracy of 98%. The 3-D displacement of the reflector ball is calculated by using reflected Infrared rays from the ball and photo sensitive diodes (PSDs). More details about the design and data acquisition with $M2S2$ is provided in [23]. Two typical microsurgical tasks were performed by five surgeons and five novice subjects:

i) Pointing task: In this task, two dots were displayed on the monitor screen. One dot was white in color and fixed while the another dot was orange in color and moved according to the user's tool tip movement. Subjects were instructed to keep the orange dot overlapping the white dot for 30s.
ii) Tracing task: In this task, a circle with 4 *mm* diameter was displayed on the monitor screen. Subjects were instructed to trace the circumference of the circle in the clockwise direction as accurately as possible for 30s with a speed that is realistic for surgical manipulation tasks.

Each task was performed at three visual magnifications: 1x, 10x and 20x, and with grip force of 1 to 2 N. Sampling frequency of 250 Hz was employed.

B. PERFORMANCE MEASURES

Prediction performance of all methods is quantified by using *%Accuracy*. For 1D signals, the *%Accuracy* defined as:

$$\%Accuracy(s_x) = \frac{RMS(s_x) - RMS(e_x)}{RMS(s_x)} \times 100; \qquad (9)$$

where $RMS(s_x) = \sqrt{(\sum_{k=1}^{k=m}(s_{x,k})^2/m)}$ with m is the number of samples, $s_{x,k}$ is the x-axis input signal at instant k and e_x is the obtained estimation error with a tremor modeling method. Since we are considering modeling the tremor signal in the 3-D space, the reported *%Accuracy* is the mean value across all 3-axis, defined as

$$\%Accuracy = \frac{3DAccuracy}{3}; \qquad (10)$$

where $3DAccuracy = \%Accuracy(s_x) + \%Accuracy(s_y) + \%Accuracy(s_z)$.

C. HYPER-PARAMETER SELECTION

To identify the optimal initialization for hyper-parameters of all methods, 10 randomly selected trials from both micro-surgeon and novice subject groups are chosen. The first four seconds data (1000 samples) is considered as the training dataset and the rest 25 seconds as the testing data set. ELM-1D and LSSVM-1D formulates input vector with tremor signal in all three-axes separately. Thus, both these methods are employed on three-axes separately and the over-all prediction accuracy is computed according to (10). ELM-3D formulates the input vector by cascading all three-axes data into one single real-value vector and performs prediction for three-axis simultaneously. QELM and QwFLC formulate the input vector by representing the three-axes data into three orthogonal axes in the complex domain and then performs prediction for three-axes simultaneously.

Grid search is conducted on the training data with QELM (as shown in Fig. 2(a)) for each trace separately with a wide range of values for the L and the p as $1 \leq L \leq 200$ and $1 \leq m \leq 100$ with a step size of 10, respectively. The obtained nonlinear mapping with each combination was later employed for modeling the testing data. For each combination, RMS of prediction error obtained according to (9) is computed. The pair $(L,\ p)$ that provides the least RMS of prediction error was considered as the optimal pair for initialization. Variations in the identified hyper-parameters over the traces are not significant. Furthermore, the variations in the identified optimal parameters across the groups (surgeons and novice subjects) is negligible. Although the variations across the identified parameters are small, to obtain a unified value for initialization, we computed the mean for the identified hyper-parameters of all the traces and then considered the obtained mean as the optimal hyper-parameters for initialization. Based on the analysis conducted on 20 traces, we determined the optimal hyper-parameters of QELM and ELM as $L = 100$ and $p = 20$. For illustration, analysis on the average performance of the selected 10 trials with the whole range of $(L,\ p)$ is shown in Fig. 3. Results demonstrated

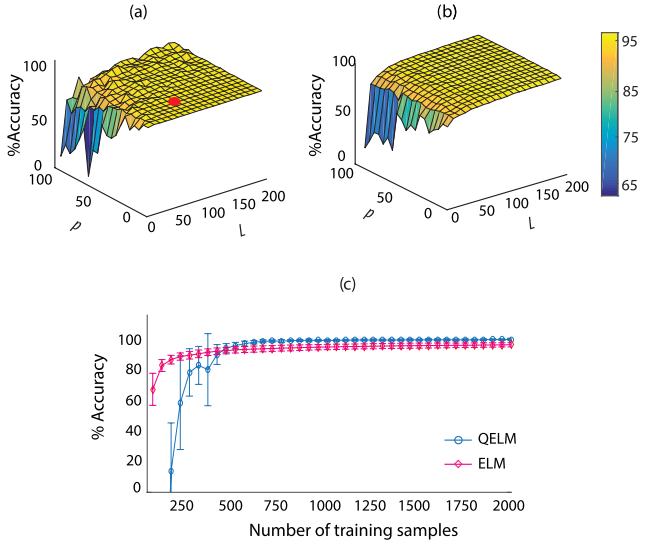

FIGURE 3. Hyper-parameter selection a) QELM, b) ELM, and c) optimal number of training samples. The color code represents %Accuracy (Mean over standard deviation) for single-step prediction error.

that the real valued ELM is robust with respect to the hyper-parameter, whereas the QELM shows a clear improvement in performance with the increased number of hidden units. The similar analysis is adopted on these trials with various number of training samples (N) to verify whether any statistically significant variations in the size of training data set are present. Results showed that the variations are not significant, as shown in Fig. 3(c). Thus, in this work, $N = 1000$ is identified as the optimal size of training set for all subjects.

The above detailed procedure is employed for identifying optimal initialization of LSSVM-1D parameters, namely regularization parameter C and Kernel parameter (γ). For QwFLC, the parameter set reported in [13] is used.

D. COMPARISON ANALYSIS

The whole motion acquired from all three axes was filtered with a zero-phase third-order Butterworth band-pass filter with a pass-band of 6 Hz to 20 Hz for this analysis to separate the tremulous motion from the voluntary motion. To model the tremor signal characteristics for multi-step prediction, we induced various delays that are in-line with the delays introduced by the digital filters. The delayed tremor signal is provided as an input to the prediction methods to perform multi-step prediction with the prediction horizon similar to that of the introduced delay. In this work, four prediction horizons are considered i.e., 4 ms, 20 ms, 40 ms, and 60 ms. With a sampling frequency of 250 Hz, the chosen horizons are equivalent to prediction of the tremor signal for 1 sample, 5 samples, 10 samples, and 15 samples ahead respectively. The predicted tremor signal was compared with the actual tremor motion to compute the prediction error, as shown in Fig. 4. Comparisons analysis was conducted on tremor data set for four prediction methods 1) QwFLC, 2) ELM-1D (real-valued one dimensional modeling with ELM), 3) ELM-3D (real-valued three dimensional modeling with ELM), and QELM. The block diagram representation of the simulation study conducted in this work is shown in Fig. 4. All these methods are quantified according to (9) and (10).

Prediction performance of QELM and ELM for 40ms (10 samples) horizon on a typical tremor motion acquired from a novice subject while performing tracing task is shown in Fig. 5. The predicted trace obtained from QELM and ELM were shown in Fig. 5(b). The estimation errors obtained

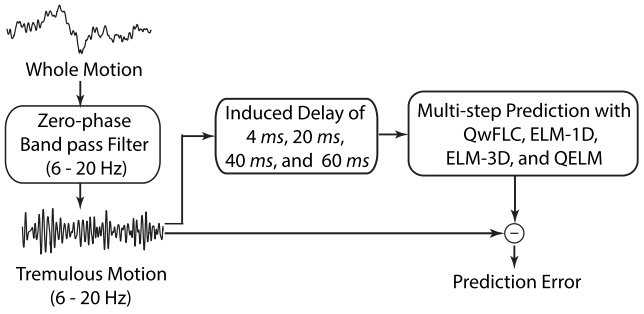

FIGURE 4. Block diagram of the simulation study.

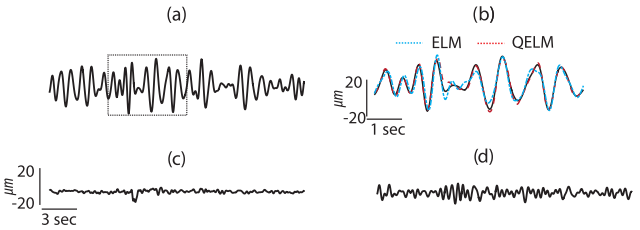

FIGURE 5. a) Tremor signal (in x-axis) from a typical novice subject in the tracing task; b) tracking performance of QELM and ELM for 40ms horizon; c) prediction error with QELM; d) prediction error with ELM.

with real-valued ELM and QELM are shown in in Fig. 5(c) and Fig. 5(d), respectively. Due to cross-dimensional coupling, QELM tracks the tremor signal characteristics more accurately compared to ELM especially when there are sudden changes in the tremor characteristics, as shown in Fig. 5(b). The reduction in prediction error obtained with QELM (Fig. 5(c)) compared to the error of ELM (Fig. 5(d)) highlights the influence of cross-dimension coupling to attain accurate tremor prediction.

All the five methods have been employed for the tremulous motion estimation (4 ms horizon) and prediction tasks (20 ms, 40 ms, and 60 ms as horizons) for all trials with the optimal hyper-parameter set. Since the QwFLC algorithm was developed mainly for the purpose of modeling the tremor signal, the results were only reported at 4 ms ahead estimation and not considered for multi-step prediction tasks. The results are shown in Fig. 6. The bar plot shows the average performance and standard error for all methods obtained with all the trials for a given task. The median accuracies for QELM, ELM-3D, ELM-1D, LSSVM-1D, and QwFLC at the horizon of 4*ms* are 98.39%, 96.36%, 96.02%, 94.39%, and 63.35% respectively. Results show that QELM outperforms real-valued counterparts LSSVM-1D, ELM-1D, & ELM-3D, and QwFLC for all prediction horizons as shown in Fig. 6.

Comparison analysis performed between the variants of ELM highlight the improvement in prediction accuracy with the quaternion domain based modeling of tremor. Scatter plots obtained with the prediction accuracy of QELM for plotted against the prediction accuracies obtained with ELM-1D and ELM-3D for all horizons and all trails are shown in Fig. 7. For example if a circle marker (blue/red) lies below the diagonal line, it denotes that QELM outperforms ELM-1D/ELM-3D. From Fig. 7, it can be seen that for most of the trials, QELM provides better prediction accuracy compared to the real-domain counterparts. The better prediction accuracy with QELM further highlights that the QELM has successfully integrated the fast learning merits of ELM and the cross-dimensional coupling from the quaternion domain.

The similar analysis performed with ELM-1D and ELM-3D show that both these methods have comparable prediction performance, as shown in Fig 8. One plausible reason is that the high-dimensional vectors in the feature space generally pose challenge for learning algorithms to

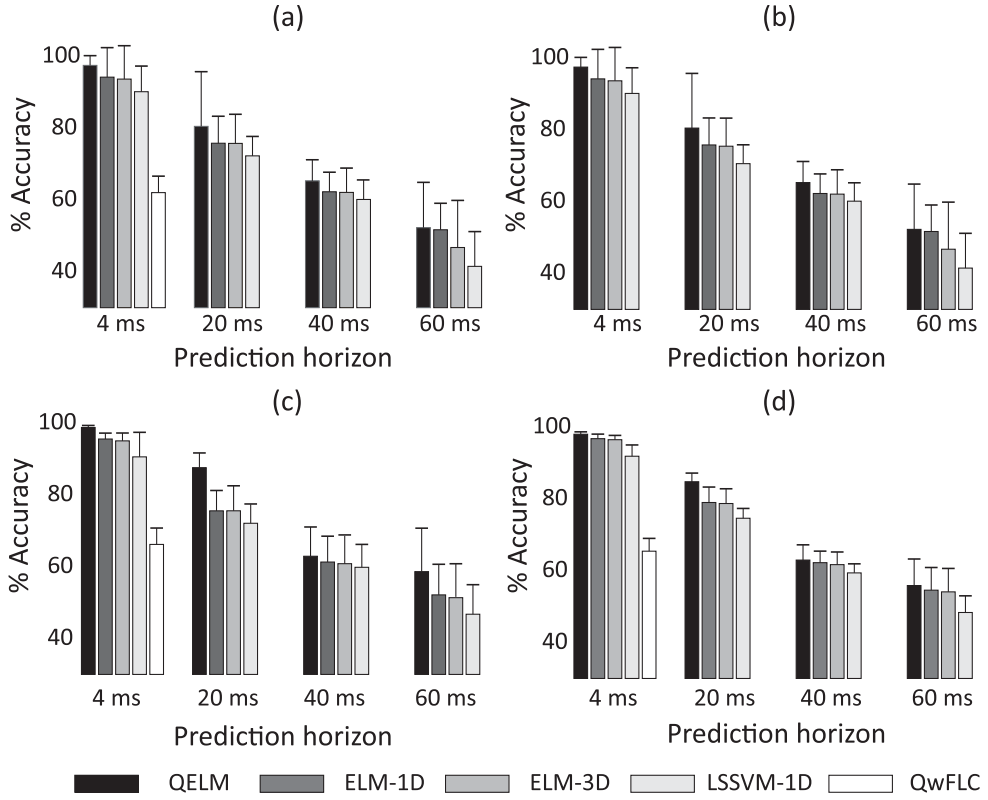

FIGURE 6. Performance comparison of QELM, ELM-1D, ELM-3D, and QwFLC for various prediction horizons. a) Surgeon poin!ng task. b) Surgeon tracing task. c) Novice pointing task. d) Novice tracing task.

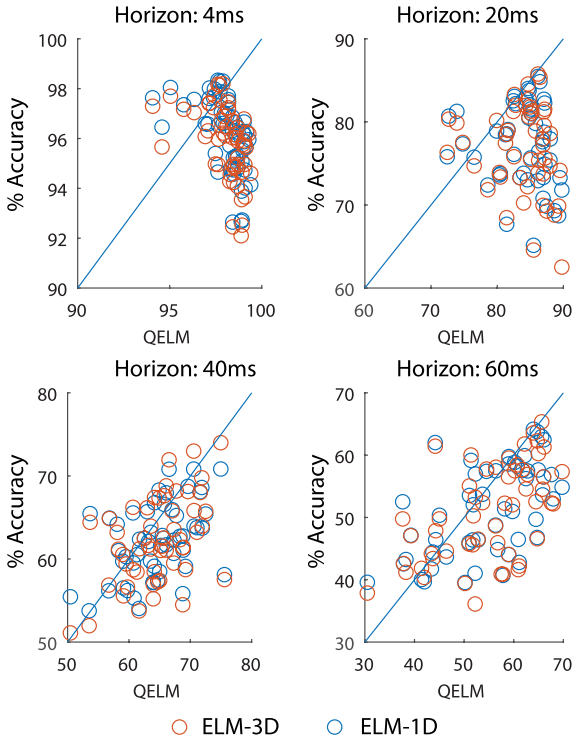

FIGURE 7. Comparison Analysis: QELM Vs ELM-1D and ELM-3D.

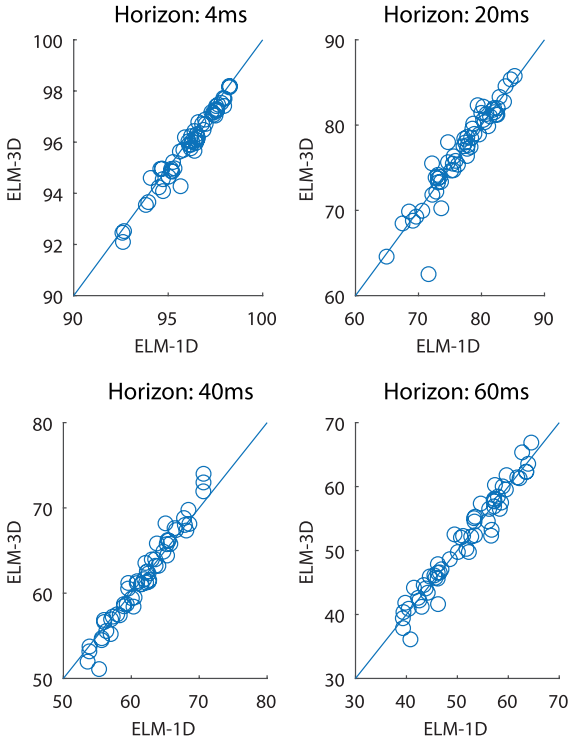

FIGURE 8. Comparison Analysis: ELM-1D Vs ELM-3D.

yield better generalization. For the tremor modeling with ELM-3D, when an input vector is formulated by cascading all three-axes information, the tremor modeling becomes a high-dimensional feature space problem. A better regularization technique is therefore required to train ELM-3D for learning a better representation of the cross-dimensional

couping in the feature space. Results obtained with QELM underpin that the modeling in quaternion domain provides better a representation of cross-dimensional coupling to learn and hence obtains a better generalization compared to ELM-3D.

All three variants of ELM outperformed the QwFLC for tremor modeling, which underscores the merits of modeling tremor motion with machine learning techniques. All the methods showed larger standard deviation in error for large prediction horizons, especially ELM-3D. With the increase in prediction horizon, hypothetically, the complexity of mapping between the input and the target increases and it hamper the performance of the employed method. The better performance of QELM as compared to its real-valued counterparts demonstrates the suitability of quaternion domain based method is suitable for modeling the tremulous motion. Comparing the results across pointing and tracing tasks, QELM showed robust performance for all prediction horizons and tasks. For completeness, we report that the QELM showed larger standard deviation in error with the surgeon group as compared to the novice subjects.

Statistical analysis (Wilcoxon sign-rank test [24]) was conducted to assess the performance of QELM, ELM-3D, ELM-1D, LSSVM-1D, and QwFLC at all the prediction horizons. In this analysis, all the traces from both pointing and tracing tasks are considered as one set for each algorithm. The total number of samples for each algorithm are thus equal to the number of trials in the experiment (N = 58). Analysis was conducted by pairing-up two prediction methods at a time. Results obtained for each pair along with the *p*-value and the effect size are tabulated in Table 1. ELM variants when paired-up with QwFLC yielded a large effect size, for example at prediction horizon of 4*ms* the effect size of 0.87 is obtained (effect size of 0.5 is generally considered as a large one). This large effect size highlights the significant improvement in prediction accuracy with ELM variants compared to the QwFLC. The pairs formed with QELM and other variants of ELM yielded large effect size irrespective of prediction horizon, this highlights that the QELM outperforms ELM-1D and ELM-3D on all prediction horizons. The pair formed with QELM and LSSVM-1D yielded similar effect-size of the pair formed with QELM and ELM variants. However, at large prediction horizons, the *p*-value of QELM is small and its effect size is almost similar to the median effect. The small effect size obtained with the pair formed by ELM-1D & ELM-3D and ELM-1D & LSSVM-1D for all prediction horizons underline the similar performance obtained with these methods.

TABLE 1. Wilcoxin sign-rank test for tremor prediction.

Horizon	Methods	Z-val	*p*-value	Effect size
4ms	QELM vs. ELM-1D	4.79	$< .001$	0.63
	QELM vs. LSSVM-1D	5.91	$< .001$	0.76
	QELM vs. ELM-3D	5.18	$< .001$	0.68
	QELM vs. QwFLC	6.62	$< .001$	0.87
	ELM-1D vs. QwFLC	6.62	$< .001$	0.87
	ELM-3D vs. QwFLC	6.62	$< .001$	0.87
	ELM-1D vs. ELM-3D	4.03	$< .001$	0.53
20ms	QELM vs. ELM-1D	5.52	$< .001$	0.72
	QELM vs. LSSVM-1D	5.78	$< .001$	0.78
	QELM vs. ELM-3D	5.59	$< .001$	0.73
	ELM-1D vs. ELM-3D	0.89	$= 0.3753$	0.12
40ms	QELM vs. ELM-1D	3.20	$= 0.001$	0.42
	QELM vs. LSSVM-1D	3.61	$= 0.001$	0.46
	QELM vs. ELM-3D	3.28	$= 0.001$	0.43
	ELM-1D vs. ELM-3D	1.13	$= 0.259$	0.15
60ms	QELM vs. ELM-1D	3.03	$= 0.002$	0.39
	QELM vs. LSSVM-1D	3.26	$= 0.001$	0.42
	QELM vs. ELM-3D	3.07	$= 0.002$	0.40
	ELM-1D vs. ELM-3D	0.22	$= 0.831$	0.03

TABLE 2. Computational Complexity for QELM, ELM-1D and ELM-3D.

	QELM	ELM-1D	ELM-3D
Training Time (ms)	276.72±5.75	20.71±4.16	5.27±0.63
Testing Time (ms)	0.94±0.23	0.02±0.02	0.01±0.02

E. RUN-TIME COMPUTATIONAL COMPLEXITY

Quaternion domain algorithms, in theory, are computationally demanding compared to its real-domain counterparts. As the tremor compensation necessitates real-time implementation, we analyzed the run-time computational complexity of all prediction algorithms to demonstrate their real-time applicability. For the sake of comparison, we used same number of training samples and hidden neurons for all algorithms. Run-time computational complexity while training phase is the time required to compute the mapping for QELM and ELM methods; whereas in testing phase the amount of time required to yield the prediction for every input sample is considered as the run-time. The experiments were conducted on a platform with Intel Core(R) i7 processor and 32GB RAM. The obtained run-time computational requirements are provided in Table 2. In line with theoretical analysis, the real-domain counterparts of ELM are approximately 10 times faster than the QELM while training phase. Training phase however need not to be computed in real-time. After identifying the mapping in training phase, the real-time applicability is governed by the run-time complexity of algorithm in testing phase. In surgical robotics applications, the hand-held instruments has a sampling period of 4ms, thus the prediction of future tremor samples must be computed in this limit. The results shown in Table 2 highlight that all methods are capable of predicting the future tremor samples within 1ms. This runtime complexity provides adequate time for compensation unit in hand-held instruments to generate the control signals for accurate compensation. This analysis demonstrates the real-time applicability of the proposed QELM algorithm for surgical robotics applications.

IV. DISCUSSIONS

Multi-step prediction with the QELM was developed in this work to counter the phase delay introduced by the digital filters. Results showed that for all the prediction horizons, the developed method yields better prediction accuracy than

existing methods. Results further highlighted that the cross-dimensional information learnt via the quaternion transformation improved the prediction accuracy compared to the real-valued variants of ELM.

The instrument (iTrem2) has a specially designed all-accelerometer inertial measurement unit to measure the instrument tool tip position in 3-DOF according to the fixed microscope reference frame [10]. For more details about the inertial measurement unit of iTrem2, refer to [10]. The tremor modeling method provides the control signal to manipulate the tip position in 3D space based on the measured tip position. The motion-space considered for the instrument is therefore three dimensional (in position domain) and hence the quaternion version of ELM is employed to model the tremor in 3-DOF position domain. However, other variants of hand-held instruments, for example Micron [8] and steady hand [25], have incorporated 6-DOF (position and orientation) sensing units. With the innate parallel processing structure of ELMs, this approach can be extended to 6-DOF modeling for other variants of hand-held instruments. However, the success of this extension to 6-DOF depends on accurate identification of the dependency across the six dimensions and the formulated of embedded space for learning.

Although the performance of the proposed QELM is superior to the real-valued variants of ELM, all these variants lack model-adaptation scheme to address the non-stationary nature of tremor. The prediction performance therefore suffers over the time, especially for large prediction horizons. Adapting to the non-stationary characteristics of tremor signal can be addressed by a sequential learning scheme. This learning scheme is readily available for real-domain variants of ELM [26]. However this scheme can not be readily extended to the quaternion domain as the universal approximation for ELM is yet to be established in the Hermitian space. With the recent progress in the theory of quaternion reproducing Kernel Hilbert space [27] and optimization in quaternion domain [28], the kernel version of the QELM will be developed for tremor modeling across the six dimensions in our future work and discussed elsewhere.

In this work, our prime focus is on physiological tremor compensation with QELM. Subsequently, the QELM method found applications in classification arena and obtained better performance compared to its real-domain counter parts [29]. As such, the QELM method can be successfully applicable to wide variety of applications such as prediction/filtering of pathological tremor [30] and estimation of physiological signals for wearable senors [31], [32] etc. Customization of QELM for these applications and for the issues therein will be discussed elsewhere.

V. CONCLUSIONS

Quaternion variant of ELM was proposed for multi-step prediction of physiological tremor to counter the phase delay induced by the digital filters in hand-held instruments. Suitability of the QELM was evaluated by considering various prediction horizons in-line with the delays of digital filters. The improvement in tremor prediction performance with QELM demonstrated that the QELM successfully integrated the fast learning merits from ELM and the cross-dimensional coupling from quaternion domain, as hypothesized. Comparison analysis and statistical tests preformed for various prediction horizons highlighted that the QELM yielded better prediction performance compared to the real-valued counterparts of ELM and other existing tremor modeling methods. Run-time computational complexity of QELM ascertain its real-time applicability.

ACKNOWLEDGMENT

(Yubo Wang and Sivanagaraja Tatinati contributed equally to this work.)

REFERENCES

[1] D. B. Camarillo, T. M. Krummel, and J. K. Salisbury, Jr., "Robotic technology in surgery: Past, present, and future," *Amer. J. Surg.*, vol. 188, no. 4, pp. 2–15, 2004.

[2] G. Deuschl, J. Raethjen, M. Lindemann, and P. Krack, "The pathophysiology of tremor," *Muscle Nerve*, vol. 24, no. 6, pp. 716–735, 2001.

[3] Z. Liu, Q. Wu, Y. Zhang, Y. Wang, and C. L. P. Chen, "Adaptive fuzzy wavelet neural network filter for hand tremor canceling in microsurgery," *Appl. Soft Comput.*, vol. 11, no. 8, pp. 5315–5329, 2011.

[4] R. J. Elbe and W. C. Koller, *Tremor*. Baltimore, MD, USA: The Johns Hopkins Univ. Press, 1985.

[5] P. E. O'Suilleabhain, and J. Y. Matsumoto, "Time-frequency analysis of tremors," *Brain*, vol. 121, no. 11, pp. 2127–2134, 1998.

[6] M. Patkin, "Ergonomics applied to the practice of microsurgery," *Austral. New Zealand J. Surg.*, vol. 47, no. 3, pp. 320–329, 1977.

[7] C. J. Payne and G.-Z. Yang, "Hand-held medical robots," *Ann. Biomed. Eng.*, vol. 42, no. 8, pp. 1594–1605, 2014.

[8] R. A. MacLachlan, B. C. Becker, J. C. Tabarés, G. W. Podnar, L. A. Lobes, Jr., and C. N. Riviere, "Micron: An actively stabilized handheld tool for microsurgery," *IEEE Trans. Robot.*, vol. 28, no. 1, pp. 195–212, Feb. 2012.

[9] W. T. Latt, U.-X. Tan, C. Y. Shee, C. N. Riviere, and W. T. Ang, "Compact sensing design of a handheld active tremor compensation instrument," *IEEE Sensors J.*, vol. 9, no. 12, pp. 1864–1871, Dec. 2009.

[10] Y. N. Aye, S. Zhao, and W. T. Ang, "An enhanced intelligent handheld instrument with visual servo control for 2-DOF hand motion error compensation," *Int. J. Adv. Robot. Syst.*, vol. 10, no. 10, pp. 1–8, 2013.

[11] K. C. Veluvolu, S. Tatinati, S.-M. Hong, and W. T. Ang, "Multistep prediction of physiological tremor for surgical robotics applications," *IEEE Trans. Biomed. Eng.*, vol. 60, no. 11, pp. 3074–3082, Nov. 2013.

[12] S. Tatinati, K. C. Veluvolu, and W. T. Ang, "Multistep prediction of physiological tremor based on machine learning for robotics assisted microsurgery," *IEEE Trans. Cybern.*, vol. 45, no. 2, pp. 328–338, Feb. 2015.

[13] K. Adhikari, S. Tatinati, W. T. Ang, K. C. Veluvolu, and K. Nazarpour, "A quaternion weighted Fourier linear combiner for modeling physiological tremor," *IEEE Trans. Biomed. Eng.*, vol. 63, no. 11, pp. 2336–2346, Nov. 2016.

[14] S. Tatinati, K. Nazarpour, W. T. Ang, and K. C. Veluvolu, "Multidimensional modeling of physiological tremor for active compensation in handheld surgical robotics," *IEEE Trans. Ind. Electron.*, vol. 64, no. 2, pp. 1645–1655, Feb. 2017.

[15] C. C. Took and D. P. Mandic, "The quaternion LMS algorithm for adaptive filtering of hypercomplex processes," *IEEE Trans. Signal Process.*, vol. 57, no. 4, pp. 1316–1327, Apr. 2009.

[16] B. Che Ujang, C. C. Took, and D. P. Mandic, "Quaternion-valued nonlinear adaptive filtering," *IEEE Trans. Neural Netw.*, vol. 22, no. 8, pp. 1193–1206, Aug. 2011.

[17] S. Tatinati, Y. Wang, and K. C. Veluvolu, "Modeling of physiological tremor with quaternion variant of extreme learning machines," in *Proc. Int. Conf. Commun. Inf. Process.*, 2016, pp. 255–258.

[18] G.-B. Huang, L. Chen, and C.-K. Siew, "Universal approximation using incremental constructive feedforward networks with random hidden nodes," *IEEE Trans. Neural Netw.*, vol. 17, no. 4, pp. 879–892, Jul. 2006.
[19] G.-B. Huang, H. Zhou, X. Ding, and R. Zhang, "Extreme learning machine for regression and multiclass classification," *IEEE Trans. Syst., Man, Cybern. B. Cybern.*, vol. 42, no. 2, pp. 513–529, Apr. 2012.
[20] J. Arvo, "Random rotation matrices," in *Graphics Gems II*. New York, NY, USA: Academic, 1991, pp. 355–356.
[21] Y. Xia, C. Jahanchahi, and D. P. Mandic, "Quaternion-valued echo state networks," *IEEE Trans. Neural Netw. Learn. Syst.*, vol. 26, no. 4, pp. 663–673, Apr. 2015.
[22] I. Kyrchei, "Explicit representation formulas for the minimum norm least squares solutions of some quaternion matrix equations," *Linear Algebra Appl.*, vol. 438, no. 1, pp. 136–152, 2013.
[23] E. L. M. Su, T. L. Win, W. T. Ang, T. C. Lim, C. L. Teo, and E. Burdet, "Micromanipulation accuracy in pointing and tracing investigated with a contact-free measurement system," in *Proc. 31st Annu. Int. Conf. IEEE EMBS*, Minneapolis, MN, USA, Sep. 2009, pp. 3960–3963.
[24] J. D. Gibbons and S. Chakraborti, *Nonparametric Statistical Inference*, F. B. Raton, Ed., 5th ed. Boca Raton, FL, USA: CRC Press, 2011.
[25] B. Mitchell *et al.*, "Development and application of a new steady-hand manipulator for retinal surgery," in *Proc. IEEE Int. Conf. Robot. Automat.*, Apr. 2007, pp. 623–629.
[26] N.-Y. Liang, G.-B. Huang, P. Saratchandran, and N. Sundararajan, "A fast and accurate online sequential learning algorithm for feedforward networks,"*IEEE Trans. Neural Netw.*, vol. 17, no. 6, pp. 1411–1423, Nov. 2006.
[27] F. A. Tobar and D. P. Mandic, "Quaternion reproducing kernel Hilbert spaces: Existence and uniqueness conditions," *IEEE Trans. Inf. Theory*, vol. 60, no. 9, pp. 5736–5749, Sep. 2014.
[28] D. Xu, Y. Xia, and D. P. Mandic, "Optimization in quaternion dynamic systems: Gradient, hessian, and learning algorithms," *IEEE Trans. Neural Networks Learn. Syst.*, vol. 27, no. 2, pp. 249–261, Feb. 2015.
[29] T. Minemoto, T. Isokawa, H. Nishimura, and N. Matsui, "Feed forward neural network with random quaternionic neurons," *Signal Process.*, vol. 136, pp. 59–68, Jul. 2017.
[30] N. Kostikis, D. Hristu-Varsakelis, M. Arnaoutoglou, and C. Kotsavasiloglou, "A smartphone-based tool for assessing parkinsonian hand tremor," *IEEE J. Biomed. Health Inform.*, vol. 19, no. 6, pp. 1835–1842, Nov. 2015.
[31] S. Tatinati, K. Nazarpour, W. T. Ang, and K. C. Veluvolu, "Ensemble framework based real-time respiratory motion prediction for adaptive radiotherapy applications," *Med. Eng. Phys.*, vol. 38, no. 8, pp. 749–757, 2016.
[32] G. Shafiq, S. Tatinati, W. T. Ang, and K. C. Veluvolu, "Automatic identification of systolic time intervals in seismocardiogram," *Sci. Rep.*, vol. 6, Nov. 2016, Art. no. 37524.

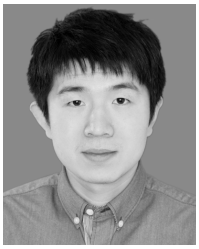

YUBO WANG (M'16) received the B.Eng. degree in electronics information engineering from Xi'an Technological University, China, in 2009, the master's degree in electrical engineering from Kyungpook National University, Daegu, South Korea, in 2011, and the Ph.D. degree from the School of Electronics Engineering, Kyungpook National University, in 2016. He is currently a Post-Doctoral Research Fellow with the School of Life Science and Technology, Xidian University. His research interests include adaptive signal estimation and machine learning algorithms for the application to bio-signal processing.

SIVANAGARAJA TATINATI (M'18) received the B.Tech. degree in electronics and communication engineering from Acharya Nagarjuna University, Guntur, India, in 2010, and the Ph.D. degree from the School of Electronics Engineering, Kyungpook National University, Daegu, South Korea, in 2016. He held a post-doctoral position at the School of Computer Science, Kyugnpook National University, in 2016. Since 2017, he has been a Research Fellow with the School of Electrical and Electronics Engineering, Nanyang Technological University, Singapore. His current research areas include machine learning, data analytics, natural language processing and generation, and robotics technology for biomedical applications.

KABITA ADHIKARI (M'14) received the B.Eng. degree in electronics and communication engineering from the Institute of Engineering Pulchowk Campus, Tribhuvan University, Kirtipur, Nepal, in 2004, and the M.Sc. degree in optoelectronics and communication systems from Northumbria University, Newcastle upon Tyne, U.K., in 2007. She is currently pursuing the Ph.D. degree with Newcastle University, Newcastle upon Tyne. From 2008 to 2010, she was a Lecturer with the South Tyneside College. She then joined Newcastle University in 2010 as a Teaching Fellow. Her research interests include biomedical signal processing and quaternion adaptive filtering.

LIYU HUANG received the B.E. degree in radio technology from the Shaanxi University of Technology in 1987, and the M.S. degree and the Ph.D. degree in biomedical engineering from Xi'an Jiaotong University, in 1993 and 2001, respectively. He is currently the Head of the Biomedical Engineering Department and a Professor with the School of Life Science and Technology, Xidian University. His research interests include neural signal processing and biomedical image processing.

KIANOUSH NAZARPOUR (S'05–M'08–SM'14) received the B.Sc. degree from the K. N. Toosi University of Technology, Tehran, Iran, in 2003, the M.Sc. degree from Tarbiat Modarres University, Tehran, in 2005, and the Ph.D. degree from Cardiff University, Cardiff, U.K., in 2008, all in electrical and electronic engineering. From 2007 to 2012, he held two post-doctoral researcher posts at the University of Birmingham and Newcastle University. In 2012, he joined Touch Bionics Inc., U.K., as a Senior Algorithm Engineer working on intelligent control of multifunctional myoelectric prostheses. In 2013, he returned to Newcastle University, where he is currently a Senior Lecturer in biomedical engineering. His research interests include intelligent sensing and biomedical signal processing and their applications in assistive technology. He received the Best Paper Award at the 3rd International Brain-Computer Interface Conference, Graz, Austria (2006), and the David Douglas Award (2006), U.K., for his work on the joint space–time–frequency analysis of the electroencephalogram signals. He is currently an Associate Editor of the *Medical Engineering and Physics* Journal in the area of biomedical signal processing.

WEI TECH ANG (S'98–M'04) received the B.E. and M.E. degrees in mechanical and production engineering from Nanyang Technological University, Singapore, in 1997 and 1999, respectively, and the Ph.D. degree in robotics from Carnegie Mellon University, Pittsburgh, PA, USA, in 2004. Since 2004, he has been with the School of Mechanical and Aerospace Engineering, Nanyang Technological University, where he is currently an Associate Professor and the Head of the Engineering Mechanics Division. His research focuses on robotics technology for biomedical applications, which include surgery, rehabilitation, and cell micromanipulation.

KALYANA C. VELUVOLU (S'03–M'06–SM'13) received the B.Tech. degree in electrical and electronic engineering from Acharya Nagarjuna University, Guntur, India, in 2002, and the Ph.D. degree in electrical engineering from Nanyang Technological University, Singapore, in 2006. From 2006 to 2009, he was a Research Fellow with the Bio-Robotics Group, Robotics Research Center, Nanyang Technological University. Since 2009, he has been with the School of Electronics Engineering, Kyungpook National University, Daegu, South Korea, where he is currently an Associate Professor. He was with the School of Mechanical and Aerospace Engineering, Nanyang Technological University, as a Visiting Professor, from 2016 to 2017. He has been a principal investigator or a co-investigator on a number of research grants funded by the National Research Foundation of Korea and other agencies. He has authored or coauthored over 100 journal and conference proceedings articles. His current research interests include nonlinear estimation and filtering, sliding mode-control, brain–computer interface, autonomous vehicles, biomedical signal processing, and surgical robotics.